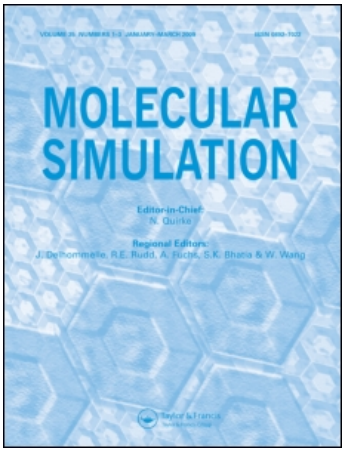

Molecular Simulation
Publication details, including instructions for authors and subscription information:
http://www.informaworld.com/smpp/title~content=t713644482

Gibbs-Ensemble Molecular Dynamics: Liquid-Gas Equilibria for Lennard-Jones Spheres and n-Hexane

M. J. Kotelyanskii[abc]; R. Hentschke[a]
[a] Max-Planck Institut für Polymerforschung, Mainz, Germany [b] N. N. Semenov Institute of Chemical Physics of the Russian Academy of Sciences, Moscow, Russia [c] Dept. of Chem. Engineering, University of Delaware, Newark, DE, USA

To cite this Article Kotelyanskii, M. J. and Hentschke, R.(1996) 'Gibbs-Ensemble Molecular Dynamics: Liquid-Gas Equilibria for Lennard-Jones Spheres and n-Hexane', Molecular Simulation, 17: 2, 95 — 112
To link to this Article: DOI: 10.1080/08927029608024099
URL: http://dx.doi.org/10.1080/08927029608024099

Molecular Simulation, 1996, Vol. 17, pp. 95–112
Reprints available directly from the publisher
Photocopying permitted by license only

GIBBS-ENSEMBLE MOLECULAR DYNAMICS: LIQUID-GAS EQUILIBRIA FOR LENNARD-JONES SPHERES AND n-HEXANE

M. J. KOTELYANSKII* and R. HENTSCHKE

Max-Planck Institut für Polymerforschung, Ackermannweg 10, 55128 Mainz, Germany

(Received June 1995, accepted September 1995)

We present a novel method to simulate phase equilibria in atomic and molecular systems. The method is a Molecular Dynamics version of the Gibbs-Ensemble Monte Carlo technique, which has been developed some years ago for the direct simulation of phase equilibria in fluid systems. The idea is to have two separate simulation boxes, which can exchange particles (or molecules) in a thermodynamically consistent fashion. Here we present the derivation of the generalized equations of motion and discuss the relation of the resulting trajectory averages to the relevant ensemble. We test this Gibbs-Ensemble Molecular Dynamics algorithm by applying it to an atomic and a molecular system, *i.e.* to the liquid-gas coexistence in a Lennard-Jones fluid and in n-hexane. In both cases our results are in good accord with previous mean field and Gibbs-Ensemble Monte Carlo results as well as with the experimental data in the case of hexane. We also show that our Gibbs-Ensemble Molecular Dynamics algorithm like other Molecular Dynamics techniques can be used to study the dynamics of the system. Self-diffusion coefficients calculated with this method are in agreement with the result of conventional constant temperature Molecular Dynamics.

KEY WORDS: Gibbs-Ensemble molecular dynamics, liquid-gas coexistence, Lennard-Jones fluid, n-hexane.

1 INTRODUCTION

Several years ago Panagiotopoulos [1] proposed the so called Gibbs-Ensemble Monte-Carlo (GEMC) technique for the direct simulation of phase coexistence in liquids and liquid mixtures. With respect to this purpose, the main advantage of the GEMC method over other techniques, such as thermodynamics integration, grand canonical Monte Carlo or Widom test particle insertion, is that each coexistence point requires only one simulation run [2]. This is achieved by actually performing two simultaneous simulations in two physically separated volumes or simulation boxes, which, however, may exchange particles such that not only the temperature but also the pressure and the chemical potential in the two volumes is the same. The original method and its modifications have been applied to numerous systems reviewed extensively in reference [2]. Certain modifications of the method have been already employed (cf. [2]) or in future studies may be employed to simulate other

*On leave from the N. N. Semenov Institute of Chemical Physics of the Russian Academy of Sciences, ul. Kosygina 4, Moscow, Russia; present address: Dept. of Chem. Engineering, University of Delaware, Newark, DE 19716-3110, USA

types of equilibria. One might for example think about fluid layers confined (or been squeezed out) between the mica surfaces of a surface force apparatus, where the temperature and the chemical potential are still the same for the confined fluid and the communicating bulk fluid, but where the pressures may be quite different. Or one might think about simulating osmotic equilibria, where one box represents a section within the interior of the osmotic cell and the other represents a section within the bulk of the reference solution. Thus far Gibbs-Ensemble simulations are mostly based on the Monte Carlo (MC) sampling method. However, Çagin [3] recently pointed out that Gibbs-Ensemble simulations based on the Molecular Dynamics (MD) technique may be useful alternatives in dense and more complicated systems, where efficient MC sampling may be difficult. Subsequently Palmer and Lo [4] presented such a MD implementation of the Gibbs-Ensemble method and applied it to a Lennard-Jones fluid.

In the following we want to discuss another Gibbs-Ensemble Molecular Dynamics (GEMD) method, which recently we introduced in a brief report, where we also simulate the liquid-gas coexistence in a simple Lennard-Jones fluid [5]. Here, however, we want to extend our GEMD method to a molecular system. One important difference between our GEMD algorithm and the suggestion of Çagin [3] and the algorithm implemented by Palmer and Lo [4] is that we do allow all the particles to be transferred between the two boxes simultaneously, not just one at a time. In addition, our algorithm does not involve a grid search for the position of the introduced particle as is used in [6]. The specific problem, which we consider here, is the liquid-gas coexistence of n-hexane, which we choose as first test for a molecular version of our GEMD method. Recent GEMC work by Smit *et al.* has focused extensively on the liquid gas coexistence in n-alkanes ranging from C_5 to C_{48} [7–9], and their work in combination with the available experimental data for short chain lengths forms a basis of comparison for our GEMD method.

The paper is structured as follows. First we describe the application of the GEMD method to the phase coexistence of a molecular one component system. Then we briefly review the previous results obtained for the liquid-gas coexistence in the limiting case of a simple Lennard-Jones fluid. In the third section we discuss the corresponding results for the case of hexane. The last section is a short conclusion.

2 METHOD

The GEMC method originally was introduced in [1] to simulate the liquid-gas coexistence of a single-component fluid system. In this case one has two physically separated volumes (or simulation boxes) whose combined volume and combined particle number is constant. Both boxes are at the same temperature and pressure. In addition they can exchange particles in a way such that the chemical potential also is the same in both boxes. For a specified temperature, and with the proper choice of the total volume, the system may phase separate so that there will be the pure liquid in one box and the pure coexisting gas in the other. This can happen below the critical temperature, when the average density corresponds to the thermodynamically unstable states below the liquid-vapor coexistence line.

In the following we develop an analogous scheme for a molecular system within the MD framework. In conventional MD one numerically solves the equations of motion for a system of N particles contained in a box of volume V having the total potential energy U. Here we consider a molecular system consisting of N atoms in M molecules, and we write the total potential energy U as a sum over inter- and intra-molecular interactions, *i.e.*

$$U = U_{\text{inter}} + U_{\text{intra}} = \sum_{\substack{i<j \\ \alpha\in i,\,\beta\in j}} \Phi(\vec{r}_{\alpha\beta}) + \sum_i U_{\text{intra}}(\{\vec{r}_{\alpha\in i}\}) \tag{1}$$

The first term, U_{inter}, is the sum over atom-atom pair potentials $\Phi(\vec{r}_{\alpha\beta})$, where $\vec{r}_{\alpha\beta} = \vec{r}_\alpha - \vec{r}_\beta$ and $\vec{r}_\alpha$ and $\vec{r}_\beta$ are the position vectors of the atoms labeled α and β belonging to two different molecules i and j. The second term, U_{intra}, is the potential energy due to all intra-molecular interactions, *i.e.* bond stretching, valence angle and torsional distortions as well as intra-molecular non-bonded interactions. In order to simulate a variable number of molecules i in each of the two boxes we introduce an extra degree of freedom ξ_i for every molecule. ξ_i can vary between 1 and 0, where $\xi_i = 1$ means that molecule i is in box 1, whereas $\xi_i = 0$ means that it is in box 2. For $1 > \xi_i > 0$ it is in a 'transition state', where it is 'felt' in both boxes. Thus, we rewrite the inter-molecular potential energy of the system as a function of the coordinates and the ξ_i as

$$\begin{aligned} U_{\text{inter}}(\{\vec{r}_\alpha\},\{\xi_i\},V_1,V_2) &= \sum_{\substack{i<j \\ \alpha\in i,\,\beta\in j}} \Phi(\vec{r}_{\alpha\beta},V_1)\xi_i\xi_j + \Phi(\vec{r}_{\alpha\beta},V_2)(1-\xi_i)(1-\xi_j)] + \sum_i g(\xi_i) \\ &= U_1 + U_2 + \sum_i g(\xi_i) \end{aligned} \tag{2}$$

where V_1 and V_2 are the volumes of the two boxes. The first two terms, U_1 and U_2, represent the inter-molecular potential energies of the first and the second box, respectively. Notice that as soon as we apply periodic boundary conditions and inter-particle interactions are calculated involving the particles closest images, the distance between them, and therefore the inter-molecular potential energy, is a function of the box dimensions (or the volume if the shape of the box is kept fixed). As in GEMC, the transfer of particles (or molecules) is controlled by the difference between their potential energies in the two boxes. The number of unphysical (but necessary) transition state molecules can be made small in comparison to the total number of molecules by introducing an additional potential function $g(\xi_i) \geqslant 0$, which is equal to zero only at $\xi_i = 0$ and at $\xi_i = 1$. In the following we use

$$g(\xi_i) = \begin{cases} w[\tanh(u\xi_i) + \tanh(u(1-\xi_i)) - 1], & 0 \leqslant \xi_i \leqslant 1 \\ \infty \quad ,\xi_i < 0 \\ \infty \quad ,\xi_i > 1 \end{cases} \tag{3}$$

This additional potential introduces a barrier of height w and steepness u between the states corresponding to the 'real' particles, *i.e.* particles or molecules which are entirely in one or the other of the two boxes (the exact definition of what this means is given below), making the transition states unfavorable.

In the case of liquid gas-coexistence in a one-component system the temperature, the pressure, and the chemical potential, even though the latter two are not explicitly specified, must be equal in the two phases and thus in the two boxes. Similar to the GEMC method this can be achieved if every change of the volume of one of the boxes is accompanied by an opposite but equal change of the volume of the other box. Thus, the total volume $V = V_1 + V_2$ of the two boxes is constant, while the individual volumes are variable. The GEMD equations of motion describing this case, as we shall see below, can be written as follows

$$
\begin{aligned}
&\vec{p}_\alpha = m_\alpha \dot{\vec{r}}_\alpha \\
&\dot{\vec{p}}_\alpha = -\frac{\partial U}{\partial \vec{r}_\alpha} - \eta \vec{p}_\alpha \\
&\dot{\eta} = \frac{1}{Q_T}\left[\sum_\alpha \frac{\vec{p}_\alpha^2}{m_\alpha} - X k_B T\right] \\
&p_{\xi_i} = m_{\xi_i} \dot{\xi}_i \\
&\dot{p}_{\xi_i} = -\frac{\partial U}{\partial \xi_i} = -\sum_{\substack{j(\neq i) \\ \alpha \in i,\, \beta \in j}} [\Phi(\vec{r}_{\alpha\beta}, V_1)\xi_j - \Phi(\vec{r}_{\alpha\beta}, V_2)(1-\xi_i)] - \sum_i \frac{\partial}{\partial \xi_i} g(\xi_i) \qquad (4) \\
&p_{V_1} = Q_P \dot{V}_1 \\
&\dot{p}_{V_1} = -\frac{\partial U}{\partial V_1} \\
&\quad = \left(\frac{\partial}{\partial V_1} \sum_{\substack{i<j \\ \alpha \in i,\, \beta \in j}} \Phi(\vec{r}_{\alpha\beta}, V_1)\xi_i \xi_j - \frac{\partial}{\partial V_2} \sum_{\substack{i<j \\ \alpha \in i,\, \beta \in j}} \Phi(\vec{r}_{\alpha\beta}, V_2)(1-\xi_i)(1-\xi_j)\right) = P_1^e - P_2^e
\end{aligned}
$$

Here $\vec{p}_\alpha$ and p_{ξ_i} are the momenta conjugate to the cartesian coordinates $\vec{r}_\alpha$ and the transfer coordinate ξ_i, respectively. η is an additional degree of freedom, and Q_T is a parameter governing the temperature relaxation. Note that the first three equations describe the evolution of a system coupled to an external heat bath with the temperature T[10], where X is a coefficient, which, as we shall see below, must be equal to the number of degrees of freedom coupled to the thermostat. Thus, if there would be only one box, this would correspond to the well known extended system NVT ensemble simulation, where the temperature of the box is controlled via a Nose-Hoover thermostat. The next two equations govern the evolution of the ξ_i and thus the transfer of the molecules between the boxes. The last two equations are the equations of motion of the box volume V_1, where p_{V_1} is a momentum variable conjugate to V_1, and Q_P is a parameter governing the volume relaxation. Thus, the volume changes are controlled by the difference between the instantaneous values of the 'external' pressures P_1^e and P_2^e in the two boxes. Here, for each box, we employ the (single-box) constant-pressure MD algorithm proposed in reference [11], *i.e.* if again there would be only one box, say the first box, the equations $p_{V_1} = Q_P \dot{V}_1$ and $\dot{p}_{V_1} = P_1^e - P$ would be identical to the equations of motion derived for the box volume in reference [11] (cf. also equation (16) in reference [12]), where P is just the

preassigned pressure, which here is replaced by the instantaneous external pressure P_2^e in the second box. In this algorithm the $\vec{r}_\alpha$ are not scaled by the box dimensions and they are not mapped back into the box according to the boundary conditions whenever a particle leaves the primary box and enters one of the surrounding image boxes. The coupling to the volume fluctuations rather happens through the positions of the image particles, which is an advantage in the present context. In order to show that $P_1^e - P_2^e = -\partial U/\partial V_1$ we must realize first that

$$\frac{\partial U}{\partial V_1} = \frac{\partial U_1}{\partial V_1} + \frac{\partial U_2}{\partial V_1} = \frac{\partial U_1}{\partial V_1} - \frac{\partial U_2}{\partial V_2} \tag{5}$$

Secondly, considering for simplicity the first box only, the inter-molecular atom-atom interaction energy is

$$\Phi(\vec{r}_{\alpha\beta}, V_1)\xi_i\xi_j = \Phi(\vec{r}_\alpha - \vec{r}_\beta - \vec{R}_{1,n})\xi_i\xi_j \tag{6}$$

where

$$\vec{R}_{1,n} = V_1^{1/3}(n_x, n_y, n_z) \tag{7}$$

is a vector, which maps the separation of the coordinates $\vec{r}_\alpha$ and $\vec{r}_\beta$ into the proper distance between the atoms α and β according to the minimum image convention (assuming a cubic box). The n_x, n_y, n_z are integers. Because it is only $\vec{R}_{1,n}$ which depends on V_1, we can write

$$\delta U_1 = \sum_{\substack{i>j \\ \alpha\in i,\, \beta\in j}} \vec{\nabla}_{r_{\alpha\beta}} \Phi(\vec{r}_{\alpha\beta}, V_1)\xi_i\xi_j\delta\vec{R}_{1,n} \tag{8}$$

and thus

$$\frac{\delta U_1}{\delta V_1} = \sum_{\substack{i>j \\ \alpha\in i,\, \beta\in j}} \frac{1}{3V_1}\left(\vec{\nabla}_{r_{\alpha\beta}} \Phi(\vec{r}_{\alpha\beta}, V_1)\xi_i\xi_j\vec{R}_{1,n}\right) = P_1^e \tag{9}$$

However, this is just equation (21) in reference [11] for the instantaneous external pressure (where of course $\xi_i = \xi_j = 1$). The same argument applies to the second box.

To analyze the thermodynamic properties of the ensemble described by the above set of equations of motion, we use the same arguments as were used by Hoover in the context of a constant temperature MD algorithm [10]. In the present case the generalized Liouville's equation, which describes the evolution of the phase space density distribution as a function of time, including the flow along the V_1, η, and ξ_i directions, is

$$\frac{\partial f}{\partial t} + \sum_{i,\alpha\in i} \dot{\vec{r}}_\alpha \frac{\partial f}{\partial \vec{r}_\alpha} + \dot{\vec{p}}_\alpha \frac{\partial f}{\partial \vec{p}_\alpha} + \dot{\xi}_i \frac{\partial f}{\partial \xi_i} + \dot{p}_{\xi_i} \frac{\partial f}{\partial p_{\xi_i}} + \dot{V}_1 \frac{\partial f}{\partial V_1} + \dot{p}_{V_1} \frac{\partial f}{\partial p_{V_1}} + \dot{\eta} \frac{\partial f}{\partial \eta} +$$
$$f\left(\sum_{i,\alpha\in i} \frac{\partial \dot{\vec{r}}}{\partial \vec{r}_\alpha} + \frac{\partial \dot{\vec{p}}_\alpha}{\partial \vec{p}_\alpha} + \frac{\partial \dot{\xi}_i}{\partial \xi_i} + \frac{\partial \dot{p}_{\xi_i}}{\partial p_{\xi_i}} + \frac{\partial \dot{V}_1}{\partial V_1} + \frac{\partial \dot{p}_{V_1}}{\partial p_{V_1}} + \frac{\partial \dot{\eta}}{\partial \eta}\right) = 0 \tag{10}$$

By direct substitution and using the above equations of motion one can see that the

following density function

$$f(\{\vec{r}_\alpha\},\{\vec{p}_\alpha\},\{\xi_i\},\{p_{\xi_i}\},V_1,p_{V_1},\eta)\propto$$
$$\exp\left[-\frac{1}{k_BT}\left(U(\{\vec{r}_\alpha\},\{\xi_i\},V_1,V_2)+\sum_{i,\alpha\in i}\left[\frac{\vec{p}_\alpha^{\,2}}{2m_\alpha}+\frac{p_{\xi i}^{\,2}}{2m_{\xi_i}}\right]+\frac{p_{V1}^2}{2Q_P}+\frac{Q_T\eta^2}{2}\right)\right] \quad (11)$$

represents an equilibrium solution, provided that X is equal to the degrees of freedom in the system, *i.e.* $X=3N-K$, where K is the number of constraints used for instance to fix bond lengths or valence angles. Thus, assuming ergodicity, trajectory averages based on the above equations of motion are equivalent to the corresponding averages calculated with this distribution.

Next we want to show that the averages obtained with f for each of the boxes are in fact equivalent to constant (μ,P,T)-ensemble averages in the thermodynamic limit, provided that the number of the particles in the transition state is small. The GEMD trajectory average of some quantity A, which depends on the coordinates and the momenta of the atoms $1,\ldots,n$ constituting the molecules $1,\ldots,m$ residing (for example) in the first box, is given by

$$\langle A\rangle_{\mathrm{GEMD}}=\frac{1}{Q'_{\mathrm{GEMD}}}\int d\xi^M dr^{3N}dp^{3N}dV_1\,A(\vec{r}_1,\ldots,\vec{r}_n,\vec{p}_1,\ldots,\vec{p}_n)$$
$$\exp\left[-\frac{1}{k_BT}\left(U(\{\vec{r}_\alpha\},\{\xi_i\},V_1)+\sum_{i,\alpha\in i}\frac{\vec{p}_\alpha^{\,2}}{2m_\alpha}\right)\right] \quad (12)$$

where

$$Q'_{\mathrm{GEMD}}=\int d\xi^M dr^{3N}dp^{3N}dV_1\exp\left[-\frac{1}{k_BT}\left(U(\{\vec{r}_\alpha\},\{\xi_i\},V_1)+\sum_{i,\alpha\in i}\frac{\vec{p}_\alpha^{\,2}}{2m_\alpha}\right)\right] \quad (13)$$

Here we have already performed the integration over η, p_{ξ_i}, and p_{V_1} and we have canceled the respective factors in the numerator and the denominator, as indicated by the primed Q'_{GEMD}. By choosing a proper w in $g(\xi_i)$ we can make the number of molecules in the transition state negligibly small. In this case we can also replace the integration over the ξ_i by the summation over all possible combinations of their values (0 or 1). Notice that for each value of m there are $M!/(m!(M\text{-}m)!)$ equivalent terms, corresponding to the same number of ways of distributing the total number of M distinguishable molecules between the two volumes. Thus $\langle A\rangle_{\mathrm{GEMD}}$ becomes

$$\langle A\rangle_{\mathrm{GEMD}}=\frac{1}{Q'_{\mathrm{GEMD}}}\sum_{m=0}^{M}\frac{M!}{m!(M-m)!}\int dV_1\,dr^{3n}dp^{3n}$$
$$A(\vec{r}_1\ldots\vec{r}_n,\vec{p}_1\ldots\vec{p}_n)\exp\left[-\frac{1}{k_BT}\left(\sum_{\substack{i>j\\ \alpha\in i,\beta\in j}}^{m}\Phi(\vec{r}_{\alpha\beta},V_1)+\sum_{i=1,\alpha\in i}^{m}U_{\mathrm{intra}}(\{\vec{r}_\alpha\})+\frac{\vec{p}_\alpha^{\,2}}{2m_\alpha}\right)\right]$$
$$\int dr^{3(N-n)}dp^{3(N-n)}\exp\left[-\frac{1}{k_BT}\left(\sum_{\substack{i>j>m\\ \alpha\in i,\beta\in j}}^{M}\Phi(\vec{r}_{\alpha\beta},V_2)+\sum_{\substack{i=m+1\\ \alpha\in i}}^{M}U_{\mathrm{intra}}(\{\vec{r}_\alpha\})+\frac{\vec{p}_\alpha^{\,2}}{2m_\alpha}\right)\right] \quad (14)$$

where the expression for Q'_{GEMD} transforms analogously. In addition, the integration over the coordinates and the momenta of the N-n atoms belonging to the M-m

molecules in the second box is just equal to $Q_{M-m,V_2,T}\ h^{3(N-n)}(M-m)!$, where $Q_{M-m,V_2,T}$ is the partition function of the isochoric-isothermal (M-m, V_2, T)-ensemble for M-m molecules consisting of a total of N-n atoms in the volume V_2 at temperature T.

Next we use that the partition function of a (M', V', T')-ensemble can be related to the partition function of the isobaric-isothermal (M', P', T')-ensemble, with the pressure P' being the average pressure in the (M', V', T')-ensemble (or vice versa – V' being the average volume in the (M', P', T')-ensemble) via a Laplace transformation with respect to V', which can be evaluated by applying the saddle-point method [13], *i.e.*

$$Q_{M',P',T'} = \sum_{V'} \exp\left(-\frac{P'V'}{k_B T'}\right) Q_{M',V',T'} = \frac{M'}{V_0}\int dv' \exp\left(-\frac{M'(P'v' + \tilde{F}(v', T'))}{k_B T'}\right)$$

$$= \exp\left(-\frac{P'\bar{V}'}{k_B T'}\right) Q_{M',\bar{V}',T'} \sqrt{M'}\left(\sqrt{\frac{2\pi\bar{v}' k_B T' \kappa}{V_0^2}} + O((M')^{-1})\right) \tag{15}$$

Here V_0 is just a basic unit of volume to render $Q_{M',P',T'}$ dimensionless [14], $\kappa = (V'\partial^2 F/\partial V'^2)^{-1}|_{\bar{V}'}$ is the compressibility, and $v' = V'/M'$ and $\tilde{F}(T', v') = F(T', M'v')/M'$ are the volume and the free energy per particle in the (M', V', T')-ensemble, respectively. Bars indicate saddle-point values. Applying this to our case, *i.e.* $\bar{V}' = V_2$, $T' = T$, $M' = M - m$, and $P' = P_2$, the pressure in the second box, we obtain

$$Q_{M-m,V_2,T} = Q_{M-m,P_2,T} \exp\left(\frac{P_2 V_2}{k_B T}\right) \frac{1}{\sqrt{M-m}}\left(\sqrt{\frac{V_0^2}{2\pi\kappa k_B T v}}(1 + O((M-m)^{-1})\right) \tag{16}$$

Finally we rewrite $Q_{M-m,P_2,T}$ in terms of $Q_{M,P_2,T}$ using

$$\exp\left(\frac{\mu_2 m}{k_B T}\right) = \frac{Q_{M-m,P_2,T}}{Q_{M,P_2,T}} \tag{17}$$

where μ_2 is the chemical potential of the molecules in the second box [15]. Now we can put everything together, *i.e.* we replace $Q_{M-m,P_2,T}$ in $\langle A\rangle_{\text{GEMD}}$ by the saddle-point approximation and subsequently express $Q_{M-m,P_2,T}$ via the above relation. Canceling the terms independent of m and n, *i.e.* $M!$, h^{3N}, $Q_{M,P_2,T} \exp(P_2 V/k_B T)$,..., between numerator and denominator, we obtain in the thermodynamic limit

$$\langle A\rangle_{\text{GEMD}} = \frac{1}{Q''_{\text{GEMD}}} \sum_{m=0}^{M} \frac{1}{m! h^{3n}} \exp\left(\frac{\mu_2 m}{k_B T}\right) \int dV_1 dr^{3n} dp^{3n} A(\vec{r}_1 \ldots \vec{r}_n, \vec{p}_1 \ldots \vec{p}_n)$$

$$\exp\left(-\frac{P_2 V_1}{k_B T}\right) \exp\left[-\frac{1}{k_B T}\left(\sum_{\substack{i>j \\ \alpha\in i,\beta\in j}}^{m} \Phi(\vec{r}_{\alpha\beta}, V_1) + \sum_{i=1,\alpha\in i}^{m}\left[U_{intra}(\{\vec{r}_\alpha\}) + \frac{p_\alpha^2}{2m_\alpha}\right]\right)\right] \tag{18}$$

as well as the corresponding expression for Q''_{GEMD}, where the double prime is just a reminder that the common factors were canceled and that we keep only the leading contribution in the limit of a large number of particles. Thus $\langle A\rangle_{\text{GEMD}}$ coincides with the average of A in the generalized constant (μ, P, T)-ensemble [16]. Notice that the average over the first box is calculated with the pressure and chemical potential of the second box, which shows the equality of these values in both boxes.

3 LIQUID-GAS EQUILIBRIUM FOR THE LENNARD-JONES SYSTEM

Before we employ the above method to simulate liquid-gas coexistence in a simple molecular fluid we want to briefly discuss its application to a simple atomic model system, *i.e.* the Lennard-Jone fluid [5]. We consider a system consisting of a total of $M = N = 250$ identical particles with unit mass interacting via the potential

$$\Phi(r) = 4\varepsilon\left(\left(\frac{\sigma}{r}\right)^{12} - \left(\frac{\sigma}{r}\right)^{6}\right) \tag{19}$$

with $\varepsilon = \sigma = 1$. In addition we cut the potential at $r = 2.5$ and shift it, so that the potential is zero for $r \geqslant 2.5$. The GEMD equations of motions were integrated numerically using the leap frog version of the Verlet algorithm [14] with a time step of 10^{-3}. A supplementary algorithm which deals with the abrupt changes in the potential $g(\xi)$ at $\xi = 0,1$ is contained in the Appendix. However, it is worth noting that because the results are not sensitive to the exact form of $g(\xi)$ high precision of the ξ-integration near $\xi = 0.1$ is not crucial. As we pointed out before, it is important to maintain a low (but non-zero) number of particles in the transition state. We find, that in our case the values w = 0.1 and u = 100 yield both reasonably fast exchange of the particles between the boxes and a low population of the transition state at the same time, *i.e.* we find that at equilibrium for more than 95% of the particles $0 < \xi_i < 10^{-4}$ or $0.9999 < \xi_i < 1$. In the following we assign the particles to the first and the second box according to these respective intervals, whereas all other particles are considered to be in the transition state. The values of the remaining parameters used here are $Q_T = Q_P = 100$, $m_i = 15$, $m_{\xi_i} = 10m_i$. The resulting liquid-gas coexistence densities as function of temperature are shown in Figure 1 together with the results of a corresponding GEMC simulation [17] and an approximate mean field calculation [18]. Note that these reference calculations refer to exactly the same system, which is important, because of the sensitivity of the results to the cut-off of the potential. As Figure 1 shows, the reference densities essentially bracket the coexistence densities obtain via the GEMD method. The GEMD densities shown in Figure 1 are obtained first for a low temperature, which then provides the initial configurations for the other temperatures.

We can also try to estimate the location of the critical point based on the simulation results. Here we follow a procedure discussed in detail in [17] and [19], whereby the critical temperature T_c^* and the critical density ρ_c^* (the star indicates reduced LJ units) can be estimated by fitting the GEMD results in the range $T^* > 0.85$ by $\rho_{\pm}^* = \rho_c^* + C_1(1 - T^*/T_c^*) \pm C_2(1 - T^*/T_c^*)^{\beta}$ (cf. also [20]). Note that here the law of rectilinear diameters $(\rho_l^* + \rho_g^*)/2 = \rho_c^* + C_1(1 - T^*/T_c^*)$ and the power law behavior $\rho_l^* - \rho_g^* = 2C_2(1 - T^*/T_c)^{\beta}$ are assumed. In addition we use the 3D Ising exponent $\beta = 0.32$ as in [17] and [19]. Thus we obtain $T_c^* = 1.097 \pm 0.004$ and $\rho_c^* = 0.327 \pm 0.004$, in rather close accord with the GEMC result $T_c^* = 1.085 \pm 0.005$ and $\rho_c^* = 0.317 \pm 0.006$ [17]. Note, however, that the temperature range on which these fits are based is of course somewhat arbitrary, and it is not quite clear how far below the critical point the above expression is still a reasonable fit. On the other hand, there is too much scatter in the simulation results at this point so that the

inclusion of higher terms in the above expansion about the critical point is not useful. A more detailed discussion of the behavior of the GEMD results in the vicinity of the critical point is given below in the context of the molecular system.

For one of the temperatures, *i.e.* $T^* = 0.9$ in Figure 1, Figure 2 illustrates the dependence of the number of LJ particles in the gas and in the transition state as well as the corresponding average reduced gas density as a function of the height w of the transfer potential in equation (3). As we pointed out before, it is important to maintain a low (but non-zero) number of particles in the transition state. Above

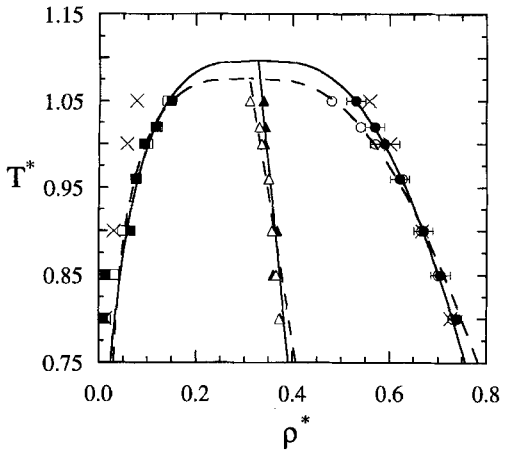

Figure 1 Reduced liquid-gas coexistence densities vs. reduced temperature, where $T^* = k_B T/\varepsilon$ and $\rho^* = \rho\sigma^3$. ρ is the number density in the respective box. Filled symbols: GEMD; hollow symbols: GEMC result of reference [17]. Circles: liquid densities; squares: gas densities; triangles: average densities. Crosses: analytical approximation of reference [18]. The error bars indicate standard deviations. The lines (solid: GEMD; dashed: GEMC) are fits as described in the text.

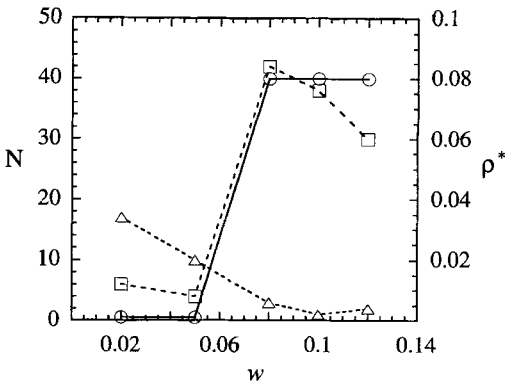

Figure 2 Average number of Lennard-Jones particles N and average reduced gas density ρ^* vs. the height of the transfer potential w for $T^* = 0.9$. Squares: N in the gas; triangles: N in the transition state; circles: gas density.

$w \approx 0.08$ the number of transition state particles, for which $0.9999 < \xi_i < 1$, is indeed small. Here the gas density assumes its proper value, which upon further increasing w does not change. It is, however, important to note that the proper magnitude of w depends on the specific system, *i.e.* for the hexane system discussed below we use $w \approx 0.05$. Whereas Figure 2 refers to the situation at the end of the respective simulation run, it is also interesting to look at the evolution of the number of particles and the densities in the two boxes. We want to do this below for the case of the molecular system.

In conclusion of this section we like to mention that we compared the results obtained with the Nose-Hoover thermostat [10] with the analogous results obtained with the thermostat proposed by Berendsen *et al.* [21]. Even though only for the former case one can prove that the algorithm does reproduce a canonical ensemble (cf. below), the obtained coexisting densities were the same within the statistical error in both cases. The second algorithm however is more stable numerically, and most of the results presented here were obtained with it. The same results were also obtained using the standard virial formula [14] for the pressure instead of the external pressure [11]. This is natural, as it was shown in reference [11] that, although the instantaneous values of the two pressures are different, their averages are the same in both cases. Finally there is a minor but noteworthy numerical point. A particle i for which for instance $\xi_i < 10^{-4}$ is considered to be a full particle in the first box. The strong divergence of the potential (19) for $r \to 0$, however, may lead to numerical artifacts if this particle's position coincides closely with the position of another particle in the second box, because according to equation (2) a particle is always 'felt' in both boxes. One way to avoid this problem, *i.e.* the collision between two full particles which are in different boxes, is to introduce a short-range 'ghost' cut-off eliminating the divergence of the potential at $r = 0$. In the present case we choose a cut-off of 0.5.

4 LIQUID-GAS COEXISTENCE OF n-HEXANE

In this section we want to consider liquid-gas coexistence in a simple molecular system. We choose a short chain alkane, n-hexane (C_6H_{14}) in our case, because n-alkanes have been considered in numerous simulation studies and there are relatively simple but still rather accurate potential functions available to model their intra- and inter-molecular interactions. Here we use the AMBER (Assisted Model Building with Energy Refinement) potential [22, 23]. We employ the 'united-atom' representation, where the CH_3- and CH_2-groups are replaced by effective LJ spheres. For the intra-molecular interactions, which include harmonic valence angle and cosine-type torsional potentials we use the tabulated AMBER force-field parameters [22, 23], whereas the lengths of the chemical bonds are kept fixed by means of the SHAKE algorithm [24]. Even though other simulations indicate that the exact form of the intra-molecular interactions are not of great importance in the present case [9], our results suggest that some care has to be taken. The inter-molecular interactions, which appear to be the most important however, are again described by means of 6–12 LJ potentials

$$\Phi(r_{\alpha\beta}) = 4\varepsilon_{\alpha\beta}\left(\left(\frac{\sigma_{\alpha\beta}}{r_{\alpha\beta}}\right)^{12} - \left(\frac{\sigma_{\alpha\beta}}{r_{\alpha\beta}}\right)^{6}\right) \tag{20}$$

cting between the 'united' atoms. Here the AMBER parameters are not adequate, and we use the parameters $\sigma_{CH_3} = \sigma_{CH_2} = 3.93$ Å, $\varepsilon_{CH_3} = 114.0$ K, $\varepsilon_{CH_2} = 47.0$ K taken from reference [8]. The parameters for the cross-interactions are calculated via the usual mixing rules $\varepsilon_{ij} = \sqrt{\varepsilon_i \varepsilon_j}$ and $\sigma_{ij} = (\sigma_i + \sigma_j)/2$. The other parameters are $Q_P = 10^4$, m_{ξ_i}, which now is equal to the mass of the molecule, $u = 100$, and $v = 0.05$. There is no explicit value for Q_T in this case, because we use the Berendsen thermostat with a relaxation time of 0.2 ps (cf. above) throughout this simulation. The above mentioned 'ghost' cut-off is 3 Å, and the total number of molecules is 144.

Figure 3 shows the liquid-gas coexistence curve obtained for this case in comparison to the experiment [25] as well as in comparison to the corresponding GEMC results [8, 9]. Both, the experimental densities and the GEMC densities, agree very well for all but the temperatures close to the critical point, where the GEMC coexistence region widens in comparison to the experiment. The open squares show our results obtained for a LJ cut-off $R_{cut} = 10$ Å, where we also shift the potential as in the case of the above LJ system. Even though the thus obtained critical temperature and density are both underestimated, this simulation shows that the GEMD methods appears to work for the simple molecular system as well. Before we address the quantitative improvement of this result, it is worth looking at the typical time evolution of the number of molecules in the two boxes as well as in the transition

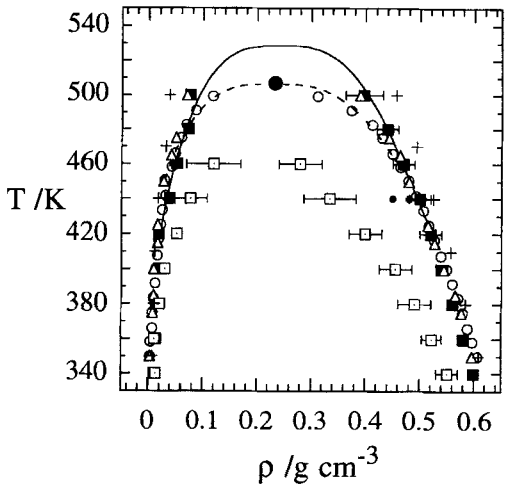

Figure 3 Liquid-gas coexistence curve for hexane. Hollow circles: experimental data of reference [25]; hollow triangles: Gibbs-Ensemble Monte Carlo result, obtained with a 13.8 Å cut-off including long-range corrections, taken from [8] and [9]. The large solid circle corresponds to the experimental critical point. Hollow squares: this work using a cut and shifted LJ potential, were the cut-off is at 10 Å; solid squares: using a 15 Å cut-off instead; small solid circles (at $T = 440$ K): liquid densities for a 12 Å and a 14 Å cut-off, respectively; plusses: result obtained for a 10 Å cut-off including long-range corrections. As in Figure 1, the error bars indicate standard deviations. These are omitted for the plusses in order to not obscure the Figure. The lines (solid: GEMD; dashed: experiment) are again fits as described in the text.

state and at the typical time evolution of the coexistence densities observed during the GEMD simulation runs.

For $T = 420$ K Figure 4 shows the number of molecules in each of the two boxes and in the transition state (left axis) as well as the actual instantaneous liquid and gas densities (right axis) as functions of time. As before we assign all molecules i for which $0 < \xi_i < 10^{-4}$ to box one and those for which $0.9999 < \xi_i < 1$ to box two. This simulation run (as well as all other runs) was started from one particular initial configuration, in which all but one of the molecules are accumulated in one of the boxes. Virtually all of the molecules then 'rush' into the transition state from which they are redistributed into the boxes. This, however, is a special feature of this initial configuration, which, if so desired, can be avoided by starting from an initial configuration closer to the final distribution (cf. the LJ system discussed above). Here both densities initially increase with time as the transition state is depopulated. Whereas the box volumes fluctuate considerably, the molecule number fluctuations are small for the above choice of parameters. For a series of temperatures the density fluctuations as a function of both time and temperature are shown in Figure 5. For low temperatures the coexistence region is wide, *i.e.*, gas and liquid densities are well seperated, and the fluctuations of the densities are small. On approaching the critical temperature the fluctuations grow. In the present case, *i.e.* for $R_{cut} = 10$ Å, $T = 500$ K corresponds to a temperature just above the critical point. Here the densities in the two boxes fluctuate strongly and no distinction is possible between liquid and gas. Thus, for the present choice of the interaction parameters the critical temperature would be close to 460 K. Due to the limited length of the simulation on which the corresponding panel in Figure 5 is based, it is of course not possible to say whether this temperature is just slightly above or below the critical temperature.

We can improve the quantitative agreement with the experimental result significantly by increasing R_{cut}. The convergence is illustrated for $T = 440$ K in Figure 3, which shows the coexistence densities for $R_{cut} = 10$, 12, 14 and 15 Å. Note that

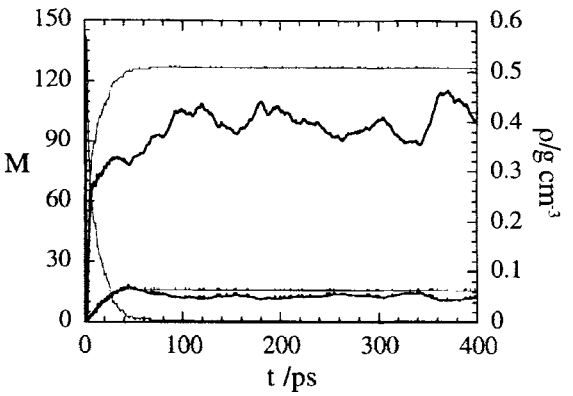

Figure 4 Number of molecules M (left axis) and density ρ (right axis) vs. time t at $T = 420$ K and $R_{cut} = 10$ Å. Upper thin line: M in the liquid box; lower thin line: M in the gas box; decreasing thin line: M in the transition state. Upper thick curve: liquid density; lower thick curve gas density.

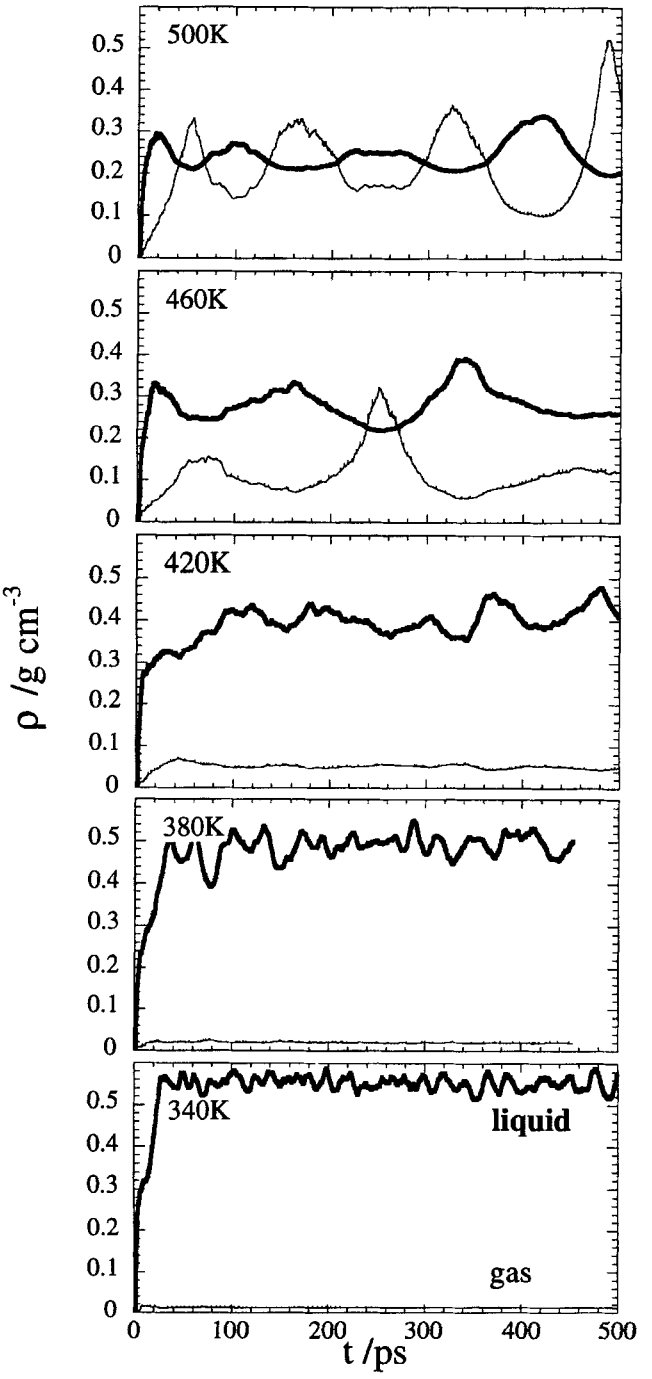

Figure 5 Densities ρ along the coexistence curve vs. time t for five different temperatures and $R_{cut} = 10$ Å (cf. open squares in Figure 3). Thick curves: liquid densities; thin curves: gas densities.

$R_{cut} = 15$ Å yields excellent quantitative agreement with the GEMC result as well as with the experiment (for $T < 480$ K). The deviations from the experiment close to criticality are to be expected, because we are using model interactions which are rather similar to those used to calculate the GEMC results. If we apply the same procedure as for the LJ fluid to the hexane densities, we can again estimate the location of the critical point. Based on the GEMD results for $T > 420$ K we obtain $T_c \approx 529$ K and $\rho_c \approx 024 \text{g/cm}^3$, whereas the location of the experimental critical point is $T_c \approx 507$ K and $\rho_c \approx 0.23 \text{g/cm}^3$.

Rather than using a large cut-off it is desirable to be able to employ the usual LJ longrange corrections [14]. These corrections modify $\dot{p}_{\xi_i} = -\partial U/\partial \xi_i$ in (4). Here we must add $-\partial(U_1^{cor} + U_2^{cor})/\partial \xi_i$ to the right-hand-side, where

$$U_1^{cor} \approx \sum_{\nu\mu} \frac{1}{2} 4\pi \frac{1}{V_1} \sum_i \xi_i \sum_j \xi_j \int_{R_{cut}}^{\infty} \Phi_{\nu\mu}(r) r^2 \, dr \tag{21}$$

and U_2^{cor} is given by an analogous expression with ξ_i replaced by $1 - \xi_i$ and V_1 replaced by V_2. Notice that the indexes ν and μ label distinct ('united') atom types in the interacting molecules i and j. The only other change affects $\dot{P}_{V_1} = P_1^e - P_2^e$ (also in (4)). Here we must add the pressure correction $P_1^{e,cor} - P_2^{e,cor}$ to the left-hand-side, where

$$P_1^{e,cor} \approx \sum_{\nu\mu} \frac{2\pi}{3} \frac{1}{V_1^2} \sum_i \xi_i \sum_j \xi_j \int_{R_{cut}}^{\infty} r^3 \frac{d\Phi_{\nu\mu}(r)}{dr} \, dr \tag{22}$$

and $P_2^{e,cor}$ is again given by an analogous equation. Using again $R_{cut} = 10$ Å (but of course without shifting the potential) and including the above long-range corrections yields the plusses in Figure 3. The coexistence region thus obtained is wider than the measured one. We attribute this to the somewhat different intra-molecular interaction terms used here in comparison to the optimized force field used in reference [9] from which we have taken the GEMC results, and where the authors also include the usual long-range corrections. It is worth mentioning in this context that we checked that as long as R_{cut} is sufficiently large (here ~ 10 Å) the results do not depend on the specific value of R_{cut}. However, another possible contribution to the discrepancy may be that the system close to criticality gets trapped in metastable states (cf. [9]).

Unlike MC, MD provides not only equilibrium thermodynamic but also dynamic quantities. To demonstrate that the present GEMD algorithm is also able to do so we calculate self-diffusion coefficients D at $T = 400$ K and $T = 460$ K in the liquid phase and compare them to self-diffusion coefficients calculated at the same temperatures and densities using conventional NVT-MD for 72 hexane molecules interacting via the same force field. The resulting atomic mean-squared displacements $\langle \Delta r^2 \rangle$ as functions of time are shown in Figure 6. The diffusion coefficients obtained via straight line fits to $\langle \Delta r^2 \rangle$ for long times using the Einstein relation (*e.g.* [14]) virtually coincide for the two methods. We obtain $D = 10.0 \cdot 10^{-9} \text{m}^2/\text{s}$ and $D = 9.9 \cdot 10^{-9} \text{m}^2/\text{s}$ at $T = 400$ K and $D = 16.2 \cdot 10^{-9} \text{m}^2/\text{s}$ and $D = 16.1 \cdot 10^{-9} \text{m}^2/\text{s}$ at $T = 460$ K for GEMD and NVT-MD, respectively.

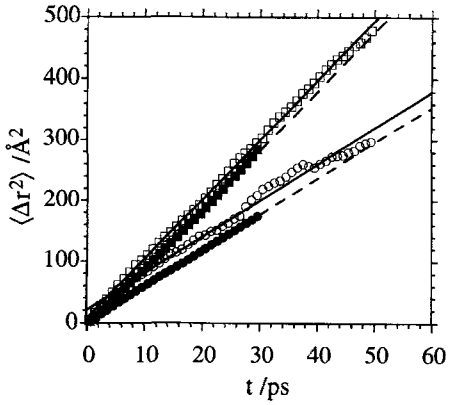

Figure 6 Mean square displacement $\langle \Delta r^2 \rangle$ of the hexane carbon atoms vs. time t calculated at coexistence in the liquid via GEMD (hollow symbols) and via NVT-MD (solid symbols) under corresponding conditions for $T = 400$ K (circles) and $T = 460$ K (squares). The lines (solid; GEMD; dashed NVT-MD) are fits to the linear range of $\langle \Delta r^2 \rangle$.

5 CONCLUSION

In this paper we have extended our GEMD algorithm previously developed for the case of a simple LJ fluid to simple molecular fluids. We find that the method gives rather good agreement with both experimental as well as GEMC results for n-hexane. We have also shown that GEMD can be used to calculate dynamic properties of the system in addition to equilibrium properties at coexistence. Our main objective here, however, was not to simulate the coexistence curve of n-hexane but rather to demonstrate that the proposed algorithm yields results, which are in qualitative and quantitative agreement with GEMC. In fact, for the case of liquid-gas coexistence, the MD approach may not necessarily have any advantage over the MC approach. After, all the additional information regarding the explicit temporal evolution of the densities and the particle exchange between the boxes may not be especially significant, because it is based, unlike in the experimental situation, on a path through an unphysical transition state. On the other hand, the MD approach may be particularly useful in complex systems, where MC move are difficult and possibly slow. Two examples of such systems were given in the introduction, *i.e.* the osmotic equilibrium between a bulk solvent and a solvent in a macromolecular network or the equilibrium between a bulk liquid and the same liquid confined between (macro-) molecular brushes. Whether GEMD possess an advantage here remains to be seen. However, the adaptation of the above algorithm for these situations is rather straightforward.

Acknowledgements

We would like to thank Dr. R. Winkler for various discussions and his help with the implementation of the constant-pressure algorithm and T. Bast for his help with

some of the numerical calculations. We are also grateful to the IPP Rechenzentrum in Garching and Dr. M. Stamm for providing part of the computer facilities used in this project. M. J. K.'s stay at the Max-Planck Institut für Polymerforschung was supported by a stipend of the Max-Planck Gesellschaft.

References

[1] A. Z. Panagiotopoulos, "Direct determination of phase coexistence properties of fluids by Monte Carlo simulation in a new ensemble", *Mol. Phys.*, **61**, 813–826 (1987).
[2] A. Z. Panagiotopoulos, "Direct determination of fluid phase equilibria by simulation in the Gibbs ensemble: A review", *Mol. Simul.*, **9**, 1–23 (1992).
[3] T. Çagin, *Molecular Dynamics methods in studying phase equilibria*; M. Doyama, J. Kihara, M. Tanaka and R. Yamamoto, Eds.; Elsevier Science Publishers B.V. (1993).
[4] B. J. Palmer and C. Lo, "Molecular dynamics implementation of the Gibbs ensemble calculation", *J. Chem. Phys.*, **101**, 10899–10907 (1994).
[5] M. J. Kotelyanskii and R. Hentschke, "Gibbs-Ensemble Molecular Dynamics: Liquid-gas equilibrium in a Lennard-Jones system", *Phys. Rev. E*, **51**, 5116–5119 (1995).
[6] T. Çagin and B.M. Petitt, "Molecular dynamics with a variable number of molecules", *Mol. Phys.*, **72**, 169–175 (1991).
[7] J. I. Siepmann, S. Karaborni and B. Smit, 'Vapor-Liquid equilibria of model alkanes", *J. Am. Chem. Soc.*, **115**, 6454–6455 (1993).
[8] J. I. Siepmann, S. Karaborni and B. Smit, "Simulating the critical behaviour of complex fluids", *Nature*, **365**, 330–332 (1993).
[9] B. Smit, S. Karaborni and J. I. Siepmann, "Computer simulations of vapour-liquid phase equilibria of n-alkanes", *preprint* (1995).
[10] W. G. Hoover, "Canonical dynamics: Equilibrium phase-space distribution", *Phys. Rev.*, **31**, 1695–1697 (1985).
[11] R. G. Winkler, H. Moravitz and D. Y. Yoon, "Novel molecular dynamics simulations at constant pressure", *Mol. Phys.*, **75**, 669–688 (1992).
[12] R. G. Winkler and R. Hentschke, "*Liquid Benzene Confined between Solid Surfaces: A Constant Pressure Molecular Dynamics Study*", *J. Chem. Phys.*, **99**, 5405–5417 (1993).
[13] A. Sveshnikov and A. Tikhonov *The Theory of functions of a complex variable*, MIR Publishers: Moscow (1978).
[14] M. P. Allen and D. J. Tildesley *Computer simulation of liquids*, Claredon Press: Oxford (1990).
[15] L. D. Landau and E. M. Lifshitz *Statistical physics*, 3 ed., Pergamon Press: Oxford, Vol. 5 (1980).
[16] T. L. Hill *Statistical mechanics*, Dover Publications: New York (1987).
[17] B. Smit, "Phase diagrams of Lennard-Jones fluids", *J. Chem. Phys.*, **96**, 8639–8640 (1992).
[18] J. G. Powles, "The liquid-vapour coexistence line for Lennard-Jones-type fluids", *Physica*, **A**, **126**, 289–299 (1984).
[19] B. Smit and C. P. Williams, "Vapour-liquid equilibria for quadrupolar Lennard-Jones fluids", *J. Phys.: Codens. Matter*, **2**, 4281–4288 (1990).
[20] L. Vega, E. deMiguel and L. F. Rull, "Phase equilibria and critical behavior of square-well fluids of variable width by Gibbs ensemble Monte Carlo simulation", *J. Chem. Phys.*, **96**, 2296–2305 (1992).
[21] H. J. C. Berendsen, J. P. M. Postma, W. F. van Gunsteren, A. DiNola and J.R. Haak, "Molecular dynamics with coupling to an external bath", *J. Chem. Phys.*, **81**, 3684–3690 (1984).
[22] S. J. Weiner, P. A. Kollman, D. A. Case, U. C. Singh, C. Ghio, G. Alagona, S. Profeta and P. Weiner, "A new force field for molecular mechanical simulation of nucleic acids and proteins", *J. Am. Chem.Soc.*, **106**, 765–784 (1984).
[23] S. Weiner, P. Kollman, D. T. Nguyen and D. A. Case, "An all atom force field for simulations of proteins and nucleic acids", *J. Comp. Chem.*, **7**, 230–252 (1986).
[24] W. F. van Gunsteren and H. J. C. Berendsen, "Algorithms for macromolecular dynamics and constraint dynamics", *Mol. Phys.*, **34**, 1311–1327 (1977).
[25] B. D. Smith and R. Srivastava *Thermodynamics Data for Pure Compounds: Hydrocarbons and Ketones*, Elsevier: Amsterdam (1986).

APPENDIX

In this appendix we discuss the modification of the integration scheme for reflection from the rigid wall in ξ-direction. The additional potential function $g(\xi)$ defined in equation (3) introduces two hard walls at $\xi = 0$ and $\xi = 1$, and its derivative is not continuous at these points. Therefore, the Verlet leap-frog scheme for "smooth" potentials, which we use to integrate the equations of motion (4), must be modified in the case of ξ during an encounter with a wall.

Consider the motion of a particle i along the ξ_i direction. Its value at the $n+1$-st step, $\xi_i(t_n + \Delta t)$, where t is the time and Δt is the time step, can be written as

$$\xi_i(t_n + \Delta t) = \xi_i(t_n) + \dot{\xi}_i(t_n)\Delta t + \int_0^{\Delta t} d\tau \int_0^{\tau} d\tau' \ddot{\xi}_i(t_n + \tau') \tag{A.1}$$

where the dots indicate time derivatives. If between t_n and $t_n + \Delta t$ particle i collides with the wall then $\xi_i(t_n + \Delta t)$ would be outside the interval $(0, 1)$ unless a δ-function type force act on it and reverses its velocity. $\ddot{\xi}_i$ here contains two contributions, *i.e.*, $\ddot{\xi}_i$ due to the smooth part of the potential and the δ-function contribution describing the collision with the wall. Let $t_n + \tau_w$ be the time when the particle reaches the wall, *i.e.* $\xi_i(t_n + \tau_w)$ is equal to either 1 or 0. Then the above formula becomes

$$\xi_i(t_n + \Delta t) = \xi_i(t_n) + \dot{\xi}_i(t_n)\Delta t + \int_0^{\Delta t} d\tau \int_0^{\tau} d\tau' \ddot{\xi}_i(t_n + \tau') + A(\Delta t - \tau_w) \tag{A.2}$$

with $A = -2\dot{\xi}_i(t_n + \tau_w)$. This expression is exact. To construct the numerical integration scheme, we expand the acceleration and velocities in Taylor series around their values at the n-th step, *i.e.*,

$$\ddot{\xi}_i(t_n + \tau') = \ddot{\xi}_i(t_n) + \dddot{\xi}_i(t_n)\tau' + O(\tau'^2) \tag{A.3}$$

and

$$\dot{\xi}_i(t_n + \tau_w) = \dot{\xi}_i(t_n) + \ddot{\xi}_i(t_n)\tau_w + \frac{1}{2}\dddot{\xi}_i(t_n)\tau_w^2 + O(\tau_w^3) \tag{A.4}$$

Performing the integration in (A.2) using (A.3) and (A.4) we obtain

$$\begin{aligned}\xi_i(t_n + \Delta t) = \xi_i(t_n) + \dot{\xi}_i(t_n)\Delta t + \frac{1}{2}\ddot{\xi}_i(t_n)\Delta t^2 + \frac{1}{6}\dddot{\xi}_i(t_n)\Delta t^3 \\ - 2(\Delta t - \tau_w)(\dot{\xi}_i(t_n) + \ddot{\xi}_i(t_n)\tau_w) - (\Delta t - \tau_w)\dddot{\xi}_i(t_n)\tau_w^2 + O(\Delta t^4)\end{aligned} \tag{A.5}$$

The last two terms in equation (A.5) describe the contribution from the wall. This expression shows, that we are left with two options. Either we evaluate the third order derivative, which is necessary if we want to preserve the fourth-order accuracy of the Verlet algorithm, or we sacrifice one order of accuracy. Here we prefer the latter, because it does not led to additional force evaluations nor does it introduce extra memory requirements. Thus, whenever a collision with the wall occurs, we switch to the third-order algorithm for one step to calculate the new values of $\xi_i(t_n + \Delta t)$ and the corresponding velocity. Equations for the third order scheme are

obtained easily from equation (A.5) by dropping all $O(\Delta t^3)$-terms. After some rearrangements they assume the form

$$\xi_i(t_n + \Delta t) = \xi_i(t_n) + \dot{\xi}_i(t_n)\tau_w + \frac{1}{2}\ddot{\xi}_i(t_n)\tau_w^2 - (\Delta t - \tau_w)(\dot{\xi}_i(t_n) + \ddot{\xi}_i(t_n)\tau_w) + \frac{1}{2}(\Delta t - \tau_w)^2\ddot{\xi}_i(t_n) \tag{A.6}$$

describing a particle, which is reflected elastically from the wall at time $t_n + \tau_w$ and subsequently travels with the acceleration $\ddot{\xi}_i(t_n)$. First we calculate $\dot{\xi}_i(t_n + \tau_w)$, *i.e.* the ξ_i-velocity at the collision,

$$\dot{\xi}_i(t_n + \tau_w)^2 = 2\ddot{\xi}_i(t_n)(\xi_i(t_n - \Delta t) - \xi_i(t_n + \tau_w)) + \dot{\xi}_i(t_n - \Delta t)^2 \tag{A.7}$$

and the time to collision τ_w after the n-th step

$$\tau_w = -\frac{1}{\ddot{\xi}_i(t_n)}(\dot{\xi}(t_n) - \dot{\xi}_i(t_n + \tau_w)) \tag{A.8}$$

where $sign[\dot{\xi}_i(t_n + \tau_w)]$ is chosen according to whether the particle is reflected towards the positive or towards the negative ξ-direction. Now we can simply write the new ξ_i and $\dot{\xi}_i$ as

$$\xi_i(t_n + \Delta t) = \xi_i(t_n + \tau_w) + \dot{\xi}_i(t_n + \tau_w)(\Delta t - \tau_w) + \frac{1}{2}\ddot{\xi}_i(t_n)(\Delta t - \tau_w)^2 \tag{A.9}$$

and

$$\dot{\xi}_i(t_n + \Delta t) = \dot{\xi}_i(t_n + \tau_w) + \ddot{\xi}_i(t_n)(\Delta t/2 - \tau_w) \tag{A.10}$$

Notice, that in order to switch back to the leap-frog Verlet algorithm $\dot{\xi}_i(t_n + \Delta t)$ is taken as the ξ_i-velocity at the half step.